Open access • Journal Article • DOI:10.1366/000370203321165179

Influence of Temperature on Water and Aqueous Glucose Absorption Spectra in the Near- and Mid-Infrared Regions at Physiologically Relevant Temperatures

Peter Snoer Jensen, Jimmy Bak, Stefan Andersson-Engels

Published on: 01 Jan 2003 - Applied Spectroscopy (Society for Applied Spectroscopy)

Topics: Absorption spectroscopy, Atmospheric temperature range, Absorption (electromagnetic radiation), Isosbestic point and Infrared

Influence of temperature on water and aqueous glucose absorption spectra in the near- and mid-infrared regions at physiologically relevant temperatures

Jensen, PS; Bak, J; Andersson-Engels, Stefan

Published in:
Applied Spectroscopy

DOI:
10.1366/000370203321165179

2003

Influence of Temperature on Water and Aqueous Glucose Absorption Spectra in the Near- and Mid-Infrared Regions at Physiologically Relevant Temperatures

PETER SNOER JENSEN,* JIMMY BAK, and STEFAN ANDERSSON-ENGELS

Risø Nat. Lab., Denmark (P.S.J., J.B.); and University of Lund, Sweden (P.S.J., S.A.-E.)

Near- and mid-infrared absorption spectra of pure water and aqueous 1.0 g/dL glucose solutions in the wavenumber range 8000–950 cm^{-1} were measured in the temperature range 30–42 °C in steps of 2 °C. Measurements were carried out with an FT-IR spectrometer and a variable pathlength transmission cell controlled within 0.02 °C. Pathlengths of 50 μm and 0.4 mm were used in the mid- and near-infrared spectral region, respectively. Difference spectra were used to determine the effect of temperature on the water spectra quantitatively. These spectra were obtained by subtracting the 37 °C water spectrum from the spectra measured at other temperatures. The difference spectra reveal that the effect of temperature is highest in the vicinity of the strong absorption bands, with a number of isosbestic points with no temperature dependence and relatively flat plateaus in between. On the basis of these spectra, prospects for and limitations on data analysis for infrared diagnostic methods are discussed. As an example, the absorptive properties of glucose were studied in the same temperature range in order to determine the effect of temperature on the spectral shape of glucose. The change in water absorption associated with the addition of glucose has also been studied. An estimate of these effects is given and is related to the expected level of infrared signals from glucose in humans.

Index Headings: **Water absorption; Glucose absorption; Temperature dependence; Transmission cell; FT-IR; Principal component analysis; PCA; Infrared; Near-infrared.**

INTRODUCTION

The use of near- and mid-infrared spectroscopy for the characterization of compounds in biological systems is limited by the strong absorption of water. The penetration depth is short where the water absorbs strongly. For a given wavenumber, the pathlength optimizes the signal-to-noise ratio (SNR) when the water absorbance is approximately 1/ln 10.[1,2] The SNR decreases rapidly in regions of strong water absorption as the pathlength deviates from the optimal. Therefore, given a necessary depth of penetration, water limits the spectral regions that may be used for precise measurements. The absorption of water also depends strongly on temperature. This dependency is most important in spectroscopic examinations of biological systems with a high water content under experimental conditions where precise control of the temperature is unattainable. For instance, it is well known that the temperature in the extremities can be several degrees below that of the body core.[3] Temperature thus influences current and future medical applications of near- and mid-infrared spectroscopy. Two notable examples are the work on noninvasive determination of blood glucose concentration to facilitate regulation of insulin in patients suffering from the increasingly prevalent disease diabetes mellitus,[4–8] and the application of infrared lasers for medical treatment and diagnostics.[9]

The water absorption spectrum has been studied in the fields of physical chemistry and biomedical spectroscopy. Bertie and Lan[10] measured the water absorption spectrum in a wide spectral range at 25 ± 1 °C and report a compilation of the best current values at that temperature in the range 15 000–1 cm^{-1}. These authors also state that there are no reliable, detailed investigations of the variation of water absorption with temperature. Libnau et al.[11,12] studied water absorption variation with temperature using an attenuated total reflectance (ATR) cell in the wavenumber range 4000–900 cm^{-1} to determine changes in the structure of liquid water. They present spectra measured at temperatures of 2, 46, and 96 °C. Venyaminov and Prendergast[1] studied the effect of increasing temperature from 25–50 °C using a 3.5 μm transmission cell in the wavenumber ranges 4000–2600 and 2350–1430 cm^{-1}. Rahmelow and Hübner[13] studied the effect of changing temperature by 1 °C at 25 °C using a 7 μm transmission cell in the range 3000–1000 cm^{-1}. Kelly and Barlow[14] studied the effect in the wavenumber range 11 800–6250 cm^{-1} with temperatures spanning 17–45 °C to determine tissue temperature. Hazen, Arnold, and Small[15] examined the problem in the range that contains combination bands of glucose, i.e., 4800–4200 cm^{-1}, letting temperature vary within 32–41 °C. These authors showed that bandpass filtering of data could remove baseline variations caused by temperature changes in this narrow wavenumber range.

The aim of this study was to investigate the temperature dependency of water and glucose solutions in the mid- and near-infrared spectral range for future applications in the biomedical field. Our focus is on the practical consequences of temperature variations for quantitative measurement of trace components in aqueous solutions. The study is thus limited to spectral ranges outside the fundamental water bands where the penetration depth is not too limited by the strong absorption from water. Information about the spectral features in these parts of the water spectrum is useful when spectral regions are sought for quantification of small amounts of compounds such as glucose, urea, and creatinine in aqueous solutions when samples are under limited temperature control, as is the case with *in vivo* and on-line measurements.

Absorption spectra of pure water at temperatures in the range 30–42 °C in both the mid- and near-infrared region are presented. The spectral data measured in this work

Received 8 August 2002; accepted 24 August 2002.

* Author to whom correspondence should be sent.

0003-7028/03/5701-0028$2.00/0

are compared to available spectral data found in the literature measured at slightly lower temperatures. Difference spectra were calculated by subtracting the 37 °C spectrum from those measured at other temperatures. The absorption spectrum of water at 37 °C and the difference spectra have been tabulated for future use. The difference spectra can be used to extract optimal spectral regions for detection of trace organic components in aqueous solutions. We used the difference spectra to estimate the influence of temperature on the expected glucose signals in humans. Finally, it was demonstrated experimentally that features of the glucose spectrum and the underlying water absorption spectrum behave differently in the two spectral ranges when the temperature varies.

EXPERIMENTAL

Spectra were measured using a Bomem MB155 Fourier transform infrared (FT-IR) spectrometer equipped with a wide-range deuterated triglycine sulfate (DTGS) detector. For measurements in the mid-infrared region, the source was an 800 K SiC Globar. For measurements in the near-infrared region, the source was a 150 W quartz–halogen lamp. Measurements were performed at 8 cm^{-1} resolution, using coaddition of 512 double-sided (symmetrical), double-buffered scans (both forward and backward scan used), each containing 2 × 8192 points. The total acquisition time for each spectrum was 320 s. All measurements were carried out with an instrument gain setting of one. Interferograms were transferred to an Intel PII based Linux workstation for data analysis. All analysis was performed using custom routines written in ANSI C. Interferograms were apodized using a cosine window, prior to Fourier transformation, and single-beam intensity spectra were calculated using full-phase information[16] without zero-filling as:

$$I(\bar{\nu}) = C(\bar{\nu})\cos\,\Phi(\bar{\nu}) + S(\bar{\nu})\sin\,\Phi(\bar{\nu}) \qquad (1)$$

where $C(\bar{\nu})$ is the cosine and $S(\bar{\nu})$ is the sine transform of the interferogram and $\Phi(\bar{\nu})$ is the phase defined by $\tan\,\Phi(\bar{\nu}) = S(\bar{\nu})/C(\bar{\nu})$.

Transmission Cell. Samples were placed in a variable pathlength liquid transmission cell (Specac 7000) with plane parallel and uncoated ZnSe windows. The transmission cell pathlength was calibrated by the fringe method before measurements took place. The pathlength could be varied between 20 μm and 6 mm, with an accuracy of ±5 μm. This enabled optimization of the SNR, for a given wavenumber region, by adjusting the pathlength to achieve a mean absorbance level of approximately 1/ln 10. A pathlength of 50 μm was used in the mid-infrared region, although a pathlength of 20 μm optimizes the SNR in the range 1500–950 cm^{-1}. The longer pathlength was chosen to reduce interference fringes in the spectra due to multiple reflections within the cell caused by the high index of refraction of the ZnSe windows (n = 2.4) compared to that of water (n = 1.33) and to reduce the relative uncertainty of the pathlength setting. This choice minimized a systematic effect at the cost of increased noise, which was then reduced by coaddition of interferograms. A pathlength of 0.4 mm was used in the near-infrared region, providing optimal SNR in the range 5000–4000 cm^{-1}. Temperature was controlled within ±0.02 °C by a Eurotherm 4208 temperature control unit, which measured sample temperature through the cell filling port with a PT100 thermo element and heated the cell by a nichrome wire wound around the cell body. The large mass (m = 640 g) of the transmission cell caused it to be very resistant to temperature changes, providing excellent stability during the measurements. The stability was obtained at the expense of the time (1 h) required for the cell to stabilize when the temperature was changed 2 °C.

Reagents. Aqueous glucose solutions (1 g/dL) were prepared and the cell was filled the day before measurements took place, allowing air bubbles caught in the cell to diffuse and equilibrium to be reached between the alpha and beta forms of glucose, when present. Reagent grade α-D-glucose (BDH Laboratory Supplies, Poole, England) was weighed using an analytical balance and dissolved in 0.5 L distilled and de-ionized Millipore water (15 MΩ).

Experimental and Data Analytical Procedure. Four repeat measurements were taken and subsequently averaged at each of the temperatures 30, 32, 34, 36, 37, 38, 40, and 42 °C with approximately 1 h between each set. The temperature was changed without adjusting the pathlength to avoid baseline variations caused by any uncertainty in pathlength setting. An air reference spectrum was measured on an empty 1.0 mm pathlength cell after the last set of measurements on the samples took place. The long pathlength of the reference cell was chosen to eliminate interference fringes in the reference measurement by making the fringe period smaller than the chosen resolution. In each wavenumber region the absorbance spectra of pure water and glucose solutions were calculated. The spectra representing pure water were baseline corrected for the wavenumber-dependent difference in Fresnel transmission between the two ZnSe–air interfaces in the air-filled reference and the two ZnSe–water interfaces in the water-filled sample. The baseline correction was carried out by calculating the change in Fresnel transmission using the tabulated values of the index of refraction of water at 25 °C given by Bertie and Lan,[10] and a constant index of refraction of 2.4 for the ZnSe windows. This correction term was subsequently added to all the absorbance spectra. The near-infrared absorption spectra were also baseline corrected by subtraction of the mean value of the spectrum in the range 10 000–8000 cm^{-1}. These spectra were converted to molar absorptivity by dividing by the molarity of water at the relevant temperature and the transmission cell pathlength.

The variation of the glucose absorption bands with temperature was investigated by carrying out the same measurements on the 1.0 g/dL glucose solutions and by comparing the glucose absorbance spectra with those of pure water.

Principal component analysis (PCA) was used to separate the data sets into a noise part and a structure part, with the first principal components describing the systematic variation in the spectral data. This technique was used to compare the effects of temperature and the presence of glucose on the water absorption spectra. The PCA software was based on ANSI C programs using double-precision versions of subroutines from Numerical Reci-

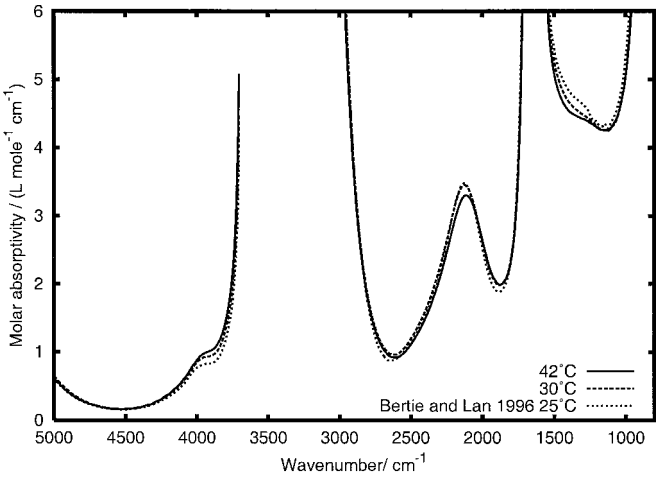

FIG. 1. Water molar absorptivity at 30 and 42 °C in the mid-infrared region. The transmission cell pathlength is 50 μm. Measurements compared with data taken from Bertie and Lan[10] measured at 25 °C.

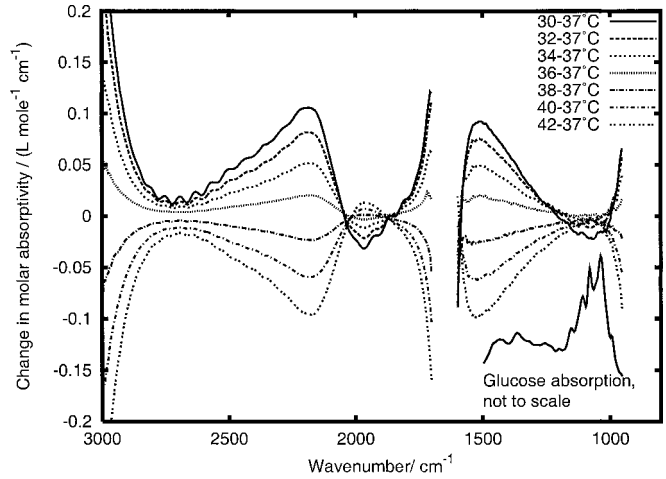

FIG. 2. Difference in water molar absorptivity with temperature around 37 °C in the mid-infrared region. The insertion shows the absorption spectrum of glucose in the region 1500–950 cm^{-1} (y-axis not to scale).

pes in C.[17] A detailed description of the PCA method can be found in the literature.[18,19]

RESULTS AND DISCUSSION

Pure Water. ***Mid-infrared Region.*** The absorption of pure water, in units of molar absorptivity, measured at 30 and 42 °C in the region 5000–950 cm^{-1} is shown in Fig. 1. The strong fundamental OH stretch and bend bands of water centered at 3500 and 1600 cm^{-1} are not resolved. In the same plot, our data are compared to the data given by Bertie and Lan,[10] measured at 25 °C. Their data agree well with our measured data, with the differences being largely systematic and following the trend indicated by the shift from 30–42 °C in our data. Given the difference in temperature and the fact that our data had been baseline corrected using Bertie and Lan's data for the refractive index of water at 25 °C, we did not expect perfect agreement. The accuracy of the pathlength setting of the transmission cell may be estimated from this agreement with the tabulated data of Bertie and Lan to be well within 2 μm. Figure 2 shows the spectra obtained by subtracting the spectrum measured at 37 °C from the spectra measured at 30, 32, 34, 36, 38, 40, and 42 °C in the range 3000–950 cm^{-1}. Data for the range 8000–3800 cm^{-1} are presented in a separate section to follow. These difference spectra are given in units of molar absorptivity and are expected to be more accurate than the absolute spectra presented in Fig. 1 since the correction for difference in Fresnel transmission, which is common to all the spectra, cancels in the subtraction. The improved accuracy of the difference spectra can be verified by the symmetry of the difference spectra around the 37 °C reference and by the coincidence of the isosbestic points in the spectrum.

The noise level of the measurements may be estimated from Fig. 3, which shows the difference spectrum of 36 °C with 37 °C as reference and the subtraction of two 37 °C spectra. These two difference spectra were obtained from one of the four repeat measurements in the 36 °C set and two of the repeat measurements in the 37 °C set. The spectra shown in Figs. 1 and 2 are averages of four such repeat measurements, and consequently, the noise level in Figs. 1 and 2 is half that shown in Fig. 3. We estimate the uncertainty to be less than 0.006 L mole^{-1} cm^{-1} in the spectral region 3000–1000 cm^{-1} (0.13% compared to the absolute value at 1200 cm^{-1}). It is observed by inspection of Fig. 3 that the noise level in most parts of the spectrum is very small compared to the spectral change caused by a change in temperature of 1 °C. In the region 1200–1000 cm^{-1}, the noise level and the change with a temperature difference of 1 °C is comparable. The 37 °C absorption spectrum and the difference spectra with 37 °C as reference are tabulated in Table I. The variations in water absorption with temperature are seen to be large on the flanks of the absorption bands and small in the local minima of the water absorption spectra. It is clear that these variations do not depend in a simple way on the absolute value of the water absorption spectrum. The ripple pattern, most clearly visible between 2800 and 2500 cm^{-1} in the 30 °C difference spectrum, is an artifact of the double reflection between the windows.

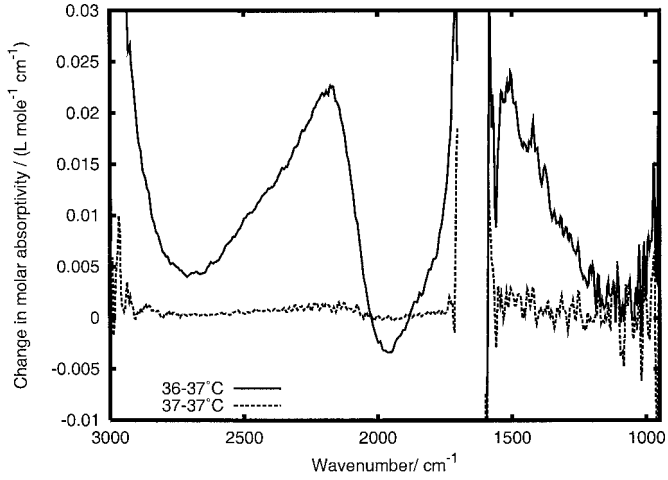

FIG. 3. Difference in water molar absorptivity of 1 °C compared to that of water at 37 °C in the mid-infrared region. Also shown is the difference between two repeat measurements of the same sample to illustrate the noise level of the measurement. Figures 1 and 2 contain data that are an average of four such repeat measurements. Accordingly, the noise level of those averaged data is half of the level shown in this figure.

TABLE I. Mid-infrared molar absorptivity of pure water at 37 °C and pure water difference spectra of 30–42 °C with 37 °C pure water as reference. The original spectra may be recovered by four-point polynomial interpolation with the following uncertainties: Difference spectra are ±0.005 L mole^{-1} cm^{-1} in the ranges 1580–960 and 2900–1700 cm^{-1}; and ±0.01 L mole^{-1} cm^{-1} in the ranges 960–950 and 3000–2900 cm^{-1}. Absolute 37 °C spectra are ±0.01 L mole^{-1} cm^{-1} in the ranges 1580–950 and 3000–1850 cm^{-1}; ±0.04 L mole^{-1} cm^{-1} in the range 1600–1580 cm^{-1}; and ±0.25 L mole^{-1} cm^{-1} in the range 1850–1700 cm^{-1}. Interpolation should be performed separately in the ranges 1600–950 and 3000–1700 cm^{-1}.

$\bar{\nu}$ cm^{-1}	37 °C L mole cm	Δ30 °C 0.01 L mole cm	Δ32 °C 0.01 L mole cm	Δ34 °C 0.01 L mole cm	Δ36 °C 0.01 L mole cm	Δ38 °C 0.01 L mole cm	Δ40 °C 0.01 L mole cm	Δ42 °C 0.01 L mole cm
960	6.026	5.562	4.548	3.306	1.123	−1.698	−4.765	−6.884
1000	5.061	−0.421	0.286	0.525	0.279	−1.047	−1.818	−2.524
1040	4.589	−1.556	−0.640	−0.135	0.014	−0.453	−0.613	−0.792
1080	4.368	−2.172	−1.057	−0.170	0.110	−0.352	−0.580	−0.294
1120	4.267	−1.724	−0.745	−0.253	−0.022	−0.493	−0.883	−0.938
1160	4.272	−0.920	−0.397	−0.032	0.105	−0.659	−0.911	−1.318
1200	4.314	−0.181	0.381	0.544	0.430	−0.622	−1.169	−1.922
1240	4.379	0.878	1.151	0.911	0.407	−0.897	−1.851	−2.763
1280	4.437	1.836	1.740	1.396	0.604	−1.036	−2.240	−3.520
1320	4.485	3.110	2.763	1.959	0.819	−1.270	−2.939	−4.534
1360	4.540	4.665	3.942	2.637	1.122	−1.501	−3.536	−5.615
1400	4.619	6.150	5.038	3.419	1.366	−1.756	−4.358	−6.905
1440	4.757	7.493	6.072	3.972	1.529	−2.160	−5.179	−8.175
1480	4.998	8.806	7.020	4.616	1.778	−2.369	−5.729	−9.078
1520	5.487	9.113	7.458	4.931	1.947	−2.651	−6.196	−9.991
1540	5.969	8.695	7.340	4.795	1.830	−2.572	−6.097	−9.652
1560	6.784	6.470	5.676	3.854	1.354	−2.457	−5.636	−8.516
1580	8.330	1.628	2.195	2.518	1.424	−2.346	−3.218	−4.529
1600	11.484	−14.393	−9.225	−9.421	−3.575	−5.385	−2.047	1.008
1700	9.315	11.525	11.446	6.353	1.225	−6.157	−10.935	−16.623
1710	7.432	11.180	9.599	6.097	1.966	−3.481	−7.995	−12.971
1720	6.012	9.164	7.639	4.999	2.151	−2.557	−6.190	−10.008
1740	4.217	5.573	4.593	3.066	1.194	−1.718	−3.988	−6.300
1760	3.241	3.712	3.062	2.027	0.836	−1.128	−2.648	−4.130
1800	2.369	1.654	1.405	1.004	0.437	−0.607	−1.362	−2.027
1840	2.067	0.043	0.213	0.289	0.204	−0.352	−0.663	−0.899
1880	1.988	−0.626	−0.433	−0.158	0.017	−0.122	−0.089	0.064
1920	2.076	−1.872	−1.254	−0.635	−0.151	0.072	0.418	0.896
1960	2.300	−3.087	−2.133	−1.135	−0.329	0.131	0.697	1.301
2000	2.641	−2.280	−1.524	−0.774	−0.203	0.019	0.316	0.670
2040	3.010	−0.419	−0.017	0.196	0.179	−0.473	−0.927	−1.429
2080	3.283	3.658	3.026	2.076	0.872	−1.174	−2.877	−4.602
2120	3.380	7.655	6.065	3.944	1.572	−1.869	−4.763	−7.678
2160	3.254	10.315	7.973	5.061	1.995	−2.297	−5.856	−9.451
2200	2.971	10.547	8.143	5.139	1.978	−2.293	−5.865	−9.444
2240	2.627	9.720	7.449	4.712	1.855	−2.107	−5.377	−8.666
2280	2.297	8.677	6.664	4.233	1.662	−1.847	−4.764	−7.644
2320	2.001	7.563	5.763	3.677	1.464	−1.649	−4.206	−6.722
2360	1.746	6.983	5.246	3.381	1.357	−1.491	−3.851	−6.046
2400	1.541	5.893	4.501	2.878	1.157	−1.284	−3.286	−5.220
2440	1.364	5.543	4.174	2.662	1.060	−1.164	−2.973	−4.732
2480	1.215	4.628	3.575	2.330	0.941	−1.048	−2.655	−4.200
2520	1.087	4.103	3.047	1.948	0.789	−0.853	−2.188	−3.437
2560	0.996	3.311	2.536	1.660	0.679	−0.718	−1.850	−2.877
2600	0.944	2.117	1.661	1.152	0.515	−0.631	−1.502	−2.321
2640	0.948	2.223	1.590	1.044	0.441	−0.469	−1.198	−1.819
2680	1.024	1.644	1.337	0.940	0.420	−0.453	−1.148	−1.747
2720	1.167	1.188	1.018	0.782	0.389	−0.537	−1.213	−1.883
2760	1.405	1.903	1.463	1.022	0.473	−0.542	−1.357	−2.110
2800	1.781	2.556	2.051	1.401	0.613	−0.721	−1.820	−2.884
2840	2.345	3.698	3.036	2.067	0.883	−1.121	−2.772	−4.484
2880	3.178	6.363	5.120	3.369	1.405	−1.728	−4.368	−7.122
2920	4.426	11.161	8.683	5.640	2.226	−2.856	−7.053	−11.604
2960	6.242	18.889	14.913	9.305	3.656	−4.510	−11.303	−18.903
3000	8.957	30.558	23.785	13.195	5.239	−8.559	−19.045	−33.430

Inspection of the difference spectra reveals that the region 1200–1000 cm^{-1} and the region 2800–2500 cm^{-1} appear to be better suited to measurement of trace component signals. These two regions show only slight broad-band variation of the water absorption with temperature. The first region changes little with temperature (less than 0.03 L mole^{-1} cm^{-1} across the 12 °C temperature difference). It is also known to contain glucose signals from the pyranose ring vibrations. The insert in Fig. 2 illustrates the position of the glucose absorption bands (y-axis, not to scale).

Near-Infrared Region. The absorption of pure water, in units of molar absorptivity, measured at 30 and 42 °C in the spectral range 8000–3800 cm^{-1} is shown in Fig.

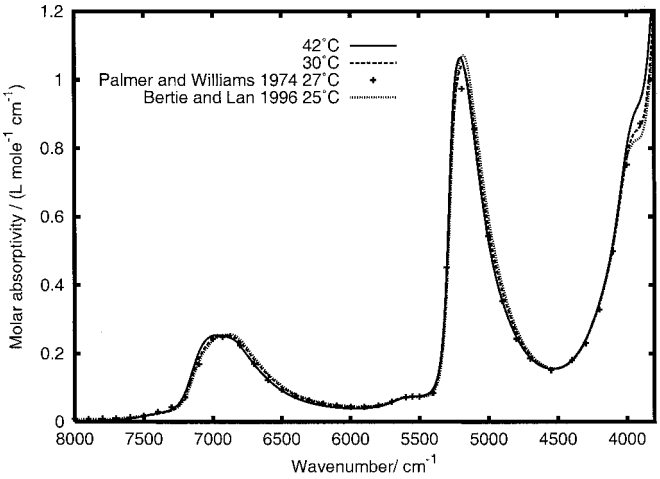

FIG. 4. Water molar absorptivity at 30 and 42 °C in the near-infrared region. The transmission cell pathlength is 0.4 mm. Measurements compared with data taken from Bertie and Lan[10] measured at 25 °C and Palmer and Williams[20] measured at 27 °C.

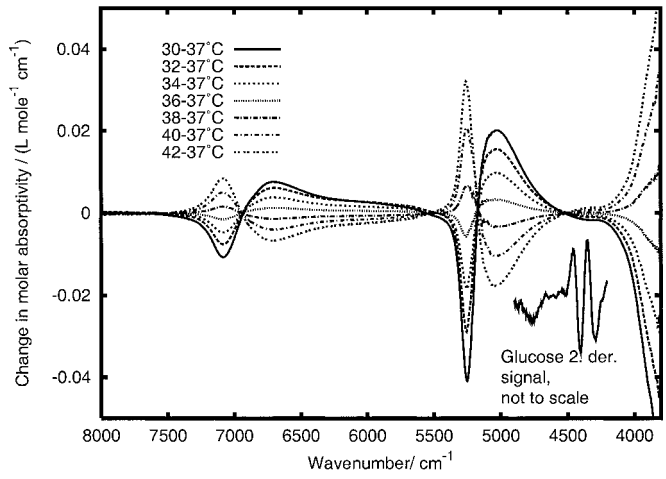

FIG. 5. Difference in water molar absorptivity with temperature around 37 °C in the near-infrared region. The insertion shows the second derivative absorption spectrum of glucose in the region 4800–4200 cm^{-1} (y-axis not to scale).

4. In the same plot, our data are compared to data measured and tabulated by other groups.[20,10] It should be noted that the data of the other groups were obtained at lower temperatures (25 and 27 °C). Good agreement exists in the major part of the spectrum, with only minor discrepancies being observed around the combination band at 5160 cm^{-1}, as previously noted by Bertie and Lan.[10] As in the mid-infrared region, our spectra were measured at a higher temperature and baseline corrected for the difference in Fresnel transmission using tabulated data on the refractive index of water at 25 °C. We thus did not expect perfect agreement.

Figure 5 displays the spectra obtained by subtracting the water spectrum measured at 37 °C from the spectra measured at temperatures 30, 32, 34, 36, 38, 40, and 42 °C. These difference spectra are given in units of molar absorptivity. Again, these difference spectra were expected to be more accurate than the absolute spectra. Their accuracy can be verified from the symmetry of the difference spectra around the 37 °C reference in Fig. 5.

The noise level may be estimated from Fig. 6, which shows the difference spectrum of 36 °C with 37 °C as reference and the subtraction of two 37 °C spectra. These two spectra were obtained from one of the four repeat measurements at 36 °C and two of the repeat measurements at 37 °C. The spectra shown in Figs. 4 and 5 are averages of four such repeat measurements, and consequently, the noise level is twice as low. The uncertainty of these difference spectra is less than 7×10^{-4} L $mole^{-1}$ cm^{-1} (0.3% compared to the absolute value at 4500 cm^{-1}). Again, it is observed that the noise level is well below the change in the spectrum induced by a change in temperature of 1 °C. In the mid-infrared region, we found a 0.13% uncertainty relative to the signal strength, which is twice as good. This finding may indicate that the mid-infrared region is better suited to measurement of trace organic components in samples where a small depth of penetration gives access to the signal from the trace component of interest.

The 37 °C absorption spectrum and the difference spectra with 37 °C as reference are tabulated in Table II. The variations in the water absorption due to temperature are observed to be of a broad-band nature. The changes are obviously highest in the vicinity of the absorption bands, with a number of isosbestic points with no temperature dependence and relatively flat plateaus in between. The isosbestic points occur close to the points in the spectrum where the water bands peak or are at a minimum. Spectral regions such as 4500–4200 and 6500–5500 cm^{-1} show a small and almost flat dependency on temperature. This explains the success of the filtering approach used by Hazen, Arnold, and Small[15,21] to remove baseline variations caused by changes in temperature.

Glucose has spectral features from overtone and combination bands in the regions mentioned above. If glucose is present in the solution, its signal will be superposed on a nearly flat baseline. The glucose signals, which contain narrow bands, may easily be separated from the broad-band variation of water using a high-pass filter.

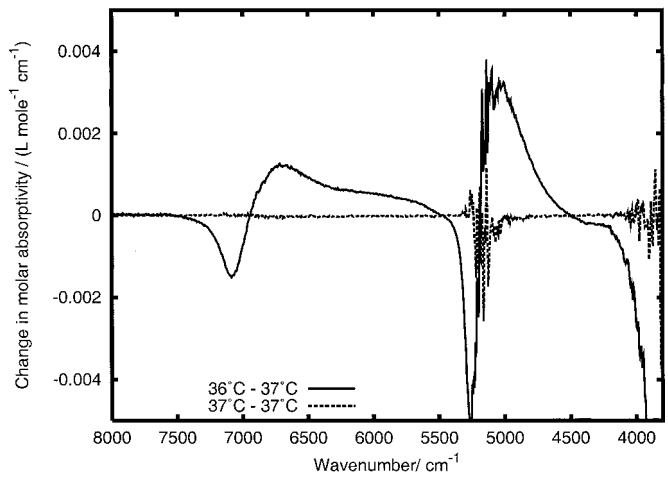

FIG. 6. Difference in water molar absorptivity of 1 °C compared to that of water at 37 °C in the near-infrared region. Also shown is the difference between two repeat measurements of the same sample to illustrate the noise level of the measurement. Figures 4 and 5 contain data that are an average of four such repeat measurements. Accordingly, the noise level of those averaged data is half the level shown in this figure.

TABLE II. Near-infrared molar absorptivity of pure water at 37 °C and pure water difference spectra of 30–42 °C with 37 °C pure water as reference. The original spectra may be recovered by four-point polynomial interpolation with the following uncertainties: Difference spectra are ±1.0 × 10^{-4} L $mole^{-1}$ cm^{-1} in the ranges 5000–4000 and 7500–5500 cm^{-1}; and ±1.5 × 10^{-3} L $mole^{-1}$ cm^{-1} in the ranges 4000–3800 and 5500–5000 cm^{-1}. Absolute 37 °C spectra are ±0.001 L $mole^{-1}$ cm^{-1} in the ranges 5000–3800 and 7500–5500 cm^{-1}; and ±0.005 L $mole^{-1}$ cm^{-1} in the range 5500–5000 cm^{-1}.

$\bar{\nu}$ cm^{-1}	37 °C L mole cm	Δ30 °C 0.01 L mole cm	Δ32 °C 0.01 L mole cm	Δ34 °C 0.01 L mole cm	Δ36 °C 0.01 L mole cm	Δ38 °C 0.01 L mole cm	Δ40 °C 0.01 L mole cm	Δ42 °C 0.01 L mole cm
3800	1.292	−6.655	−4.800	−2.832	−0.937	1.369	3.593	5.938
3840	1.044	−5.379	−3.999	−2.529	−0.872	0.839	2.713	4.570
3880	0.931	−4.492	−3.303	−2.089	−0.699	0.731	2.281	3.822
3920	0.892	−3.672	−2.684	−1.670	−0.554	0.596	1.793	3.016
3960	0.860	−2.694	−1.941	−1.203	−0.369	0.436	1.313	2.166
4000	0.790	−1.825	−1.302	−0.799	−0.251	0.277	0.855	1.424
4040	0.682	−1.203	−0.855	−0.551	−0.173	0.173	0.552	0.922
4080	0.570	−0.824	−0.581	−0.372	−0.112	0.118	0.380	0.641
4120	0.478	−0.568	−0.396	−0.256	−0.077	0.075	0.259	0.434
4160	0.406	−0.380	−0.254	−0.167	−0.050	0.048	0.166	0.288
4200	0.347	−0.254	−0.163	−0.107	−0.029	0.030	0.113	0.193
4280	0.257	−0.171	−0.103	−0.072	−0.020	0.017	0.074	0.130
4360	0.198	−0.163	−0.094	−0.067	−0.018	0.015	0.069	0.121
4440	0.167	−0.104	−0.049	−0.036	−0.007	0.006	0.042	0.073
4520	0.155	−0.008	0.025	0.009	0.008	−0.011	−0.009	−0.010
4600	0.161	0.131	0.131	0.076	0.029	−0.034	−0.080	−0.128
4680	0.183	0.342	0.290	0.175	0.061	−0.068	−0.187	−0.307
4760	0.226	0.655	0.529	0.325	0.110	−0.121	−0.347	−0.574
4840	0.295	1.096	0.861	0.533	0.178	−0.191	−0.565	−0.942
4920	0.395	1.616	1.250	0.774	0.256	−0.272	−0.820	−1.372
5000	0.549	1.979	1.527	0.955	0.320	−0.320	−1.013	−1.710
5080	0.779	1.906	1.460	0.925	0.308	−0.277	−0.939	−1.684
5160	1.015	0.417	0.557	0.340	0.121	0.003	0.006	−0.378
5200	1.051	−1.791	−1.111	−0.623	−0.180	0.411	1.228	1.342
5240	0.966	−3.878	−2.604	−1.674	−0.442	0.654	2.000	2.950
5260	0.843	−4.004	−2.856	−1.779	−0.571	0.636	2.034	3.207
5280	0.645	−3.212	−2.297	−1.453	−0.466	0.525	1.607	2.663
5300	0.437	−2.133	−1.520	−0.968	−0.315	0.340	1.072	1.796
5320	0.286	−1.275	−0.884	−0.567	−0.181	0.196	0.638	1.075
5360	0.142	−0.473	−0.288	−0.190	−0.059	0.063	0.228	0.391
5400	0.096	−0.228	−0.107	−0.074	−0.020	0.025	0.106	0.183
5480	0.076	−0.082	0.007	−0.003	0.003	−0.003	0.026	0.050
5560	0.074	0.002	0.073	0.037	0.018	−0.016	−0.016	−0.022
5640	0.068	0.096	0.145	0.080	0.031	−0.034	−0.064	−0.104
5720	0.056	0.149	0.186	0.107	0.040	−0.043	−0.092	−0.151
5800	0.046	0.184	0.213	0.124	0.045	−0.048	−0.107	−0.174
5880	0.042	0.222	0.241	0.139	0.051	−0.054	−0.125	−0.208
5960	0.041	0.252	0.265	0.154	0.054	−0.059	−0.142	−0.233
6040	0.042	0.276	0.281	0.166	0.059	−0.062	−0.152	−0.249
6120	0.046	0.300	0.297	0.177	0.063	−0.065	−0.165	−0.271
6200	0.050	0.325	0.314	0.188	0.066	−0.069	−0.175	−0.285
6280	0.057	0.358	0.335	0.199	0.069	−0.073	−0.191	−0.317
6360	0.068	0.409	0.370	0.224	0.076	−0.082	−0.218	−0.361
6440	0.082	0.487	0.422	0.258	0.088	−0.092	−0.253	−0.421
6520	0.103	0.584	0.491	0.302	0.102	−0.107	−0.304	−0.506
6600	0.130	0.682	0.563	0.350	0.119	−0.121	−0.353	−0.589
6680	0.166	0.755	0.613	0.382	0.128	−0.134	−0.394	−0.657
6760	0.207	0.716	0.582	0.364	0.123	−0.127	−0.378	−0.635
6840	0.244	0.468	0.400	0.252	0.088	−0.091	−0.270	−0.460
6920	0.254	0.075	0.111	0.071	0.029	−0.029	−0.082	−0.151
7000	0.249	−0.608	−0.400	−0.251	−0.078	0.083	0.259	0.424
7080	0.213	−1.069	−0.753	−0.469	−0.149	0.161	0.505	0.844
7120	0.175	−0.974	−0.684	−0.426	−0.137	0.147	0.460	0.773
7160	0.127	−0.714	−0.492	−0.306	−0.099	0.103	0.335	0.562
7200	0.083	−0.476	−0.318	−0.197	−0.063	0.068	0.223	0.374
7240	0.055	−0.320	−0.202	−0.125	−0.040	0.042	0.145	0.246
7320	0.032	−0.160	−0.085	−0.053	−0.017	0.015	0.060	0.105
7400	0.025	−0.097	−0.041	−0.024	−0.007	0.005	0.028	0.052
7480	0.018	−0.057	−0.013	−0.006	0.000	−0.001	0.009	0.014
7500	0.016	−0.050	−0.010	−0.003	0.000	−0.003	0.005	0.008

This is illustrated by the insert in Fig. 5, which shows the second derivative absorption spectrum of aqueous glucose in the combination band 5000–4000 cm^{-1}. The y-axis of this insert is not to scale. Figure 5 shows that quantitative *in vivo* spectroscopy will be very difficult in the vicinity of the stronger absorption bands. Realistic temperature variations close to 37 °C have an enormous impact on the appearance of the water spectrum, leaving

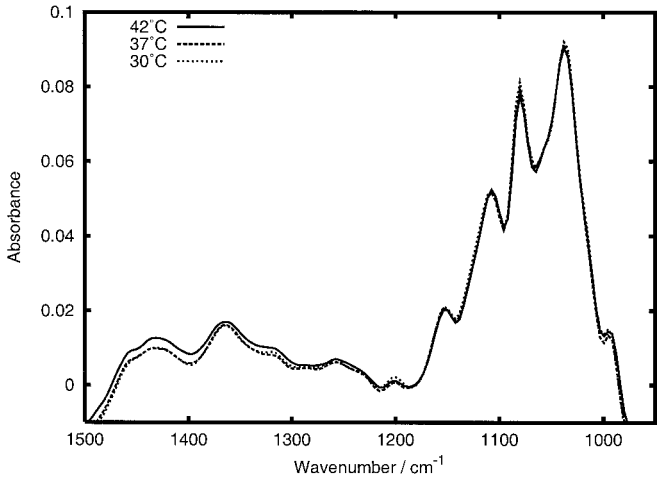

FIG. 7. Mid-infrared absorption spectrum of aqueous glucose at 1 g/dL concentration, 50 μm pathlength, at temperatures 42, 37, and 30 °C.

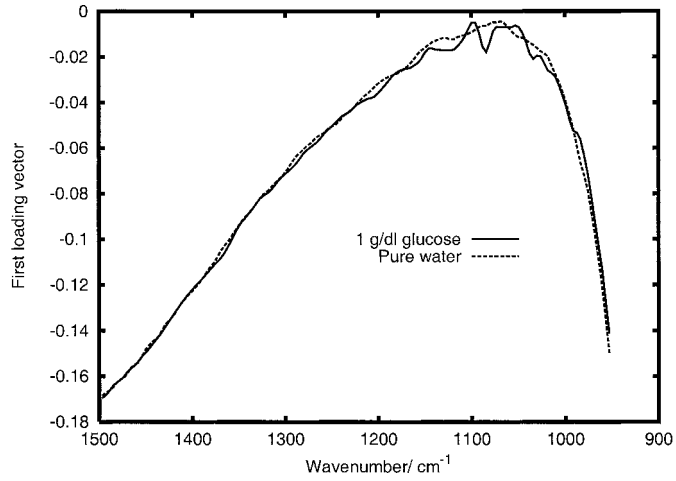

FIG. 8. First loading vector describing the change in absorbance of pure water with temperature and first loading vector describing the corresponding change in absorbance of 1 g/dL glucose solution.

only a few spectral windows open for quantitative analysis. The compounds of biomedical interest must have spectral features in these windows in order to be measured quantitatively as well as qualitatively.

Aqueous Solutions of Glucose. As mentioned in the introduction, glucose measurement is important for the control and regulation of blood glucose concentration. The direct effect of temperature on the glucose spectrum and the indirect effect of change in the underlying water spectrum were estimated for temperatures varying around 37 °C. A solution of 1 g/dL, which is a factor of ten higher than the concentrations found in blood and body liquids, was used to obtain a level of absorption well above the noise level. The various effects of temperature could then be extracted and estimated. The estimated effects were then scaled down by a factor of 10 to represent the glucose concentration of 100 mg/dL expected in body fluids.

Mid-infrared Region. The relatively weak glucose spectral features from the vibrations in the pyranose ring fall in the spectral range 1500–980 cm^{-1}. This is shown in Fig. 7, which shows the absorbance spectrum of 1 g/dL aqueous glucose at 30, 37, and 42 °C with the water absorption spectrum measured at the same pathlength and temperature subtracted. It is well known, and can also be seen in Fig. 2, that this spectral range is found between the fundamental band $\bar{\nu}_2$ (1643 cm^{-1}) and the libration band $\bar{\nu}_L$ (800–500 cm^{-1}) of water. Figures 1 and 2 also clearly show that due to its high molarity and number of broad absorption bands, water absorbs everywhere in the spectrum. The absorbance of water, at a pathlength of 50 μm, can vary from 0 to ±0.04 (relative to 37 °C) in the 1500–980 cm^{-1} spectral range within the temperature range studied here. These absorbance values are found by multiplying the data in Fig. 2 by the pathlength and molarity of water. The glucose spectrum between 1100 and 1000 cm^{-1} has the highest absorbance values (0.003–0.009, scaled to 100 mg/dL, see Fig. 7).

The insert in Fig. 2 shows that in this spectral region the influence of temperature on the water spectrum is at a minimum (±0.002 a.u. as temperature is varied from 30 to 42 °C), making it ideal for determining glucose concentration. However, the part of the glucose spectrum in the region 1200–1500 cm^{-1} has only weak features (absorbance values less than 0.002). Calculations based on the data displayed in Fig. 2 show that the change in absorbance of water in this region is between 0.01 and 0.04. Consequently it seems likely that it will be difficult to use this part of the glucose spectrum for quantitative analysis, even if the data is pretreated using methods like Fourier filtering or construction of second derivatives followed by multivariate calibration techniques.

The size of the potential matrix effects between the solvent (H_2O) and solute (glucose) and the effect of mutarotation of glucose were also examined. Figure 7 shows that the glucose spectra representing three different temperatures vary slightly in regard to the position of the glucose peaks. There is a small shift in peak height (3%) of the 1080 cm^{-1} band relative to the total band height. Figure 8 shows the first loading vectors from a separate PCA analysis of the pure water data and of the aqueous glucose data. An empty cell was used for reference measurements in both cases. These loading vectors, which describe the change in water features due to the temperature change, may be compared and useful information extracted. If matrix effects were present, a significant difference between these loading vectors would be expected. As can be seen from Fig. 8, this effect is not observed. The two loading vectors are almost identical in shape. Only small glucose features are observed in the water + glucose loading vector.

The absence of the matrix effect may be explained by the fact that the glucose spectral features originate from vibrations between atoms inside the pyranose ring. The interactions between the functional groups of glucose and the hydroxy groups in water do not influence these vibrations. The fact that the absorption features from glucose are observed in the first loading vector, which models the temperature variation, indicates that the glucose signal depends on temperature. Mutarotation in water between the two glucose anomeres designated α and β is a well-known phenomenon. We believe the loading plot reveals some of the effects of this. The PCA analysis suggests that the glucose peak at 1080 cm^{-1}, known to be specific for the β form of glucose,[22] is changed by 0.0031

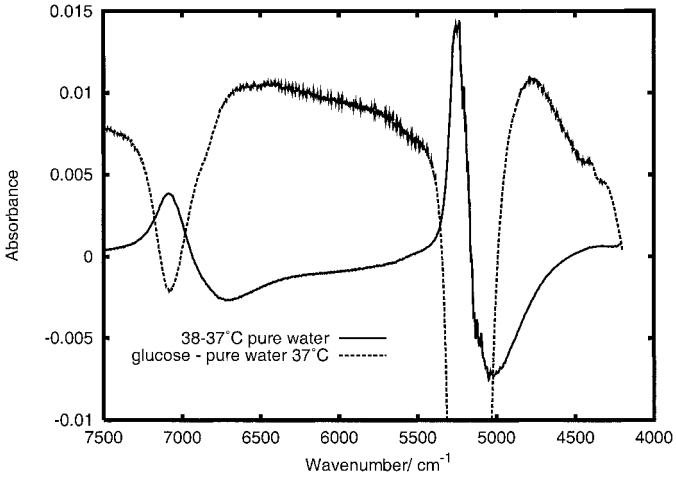

FIG. 9. Subtraction of the absorbance spectrum of pure water from the absorbance spectrum of the 1 g/dL glucose aqueous solution at 37 °C and a pathlength of 0.4 mm. The difference between two pure water absorbance spectra at 38 and 37 °C at the same pathlength is shown for comparison. Glucose specific bands are seen at 4000–4500 cm^{-1}.

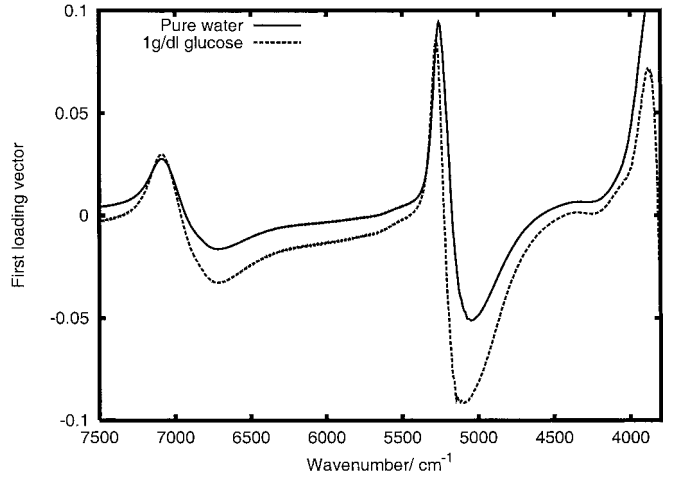

FIG. 10. First loading vector describing the change in absorbance of pure water with temperature and first loading vector describing the corresponding change in absorbance of a 1 g/dL aqueous glucose solution.

a.u. (3%). This finding confirms the estimate made from Fig. 7. The relative concentration of the two anomeres at different temperatures has been calculated from values of the equilibrium constant for the reaction given by Kendrew.[23] We calculate a 1.4% change in concentration as the temperature is varied from 30 to 42 °C, which is slightly lower than the 3% change in the signal found experimentally. These estimates show that the changes in signal due to mutarotation in the 12 °C interval are small compared to the changes in the underlying water bands.

We find that changes in the spectral features of water are the major contributors to temperature-dependent variation in the spectrum between 1500–980 cm^{-1}. The shape of the glucose spectrum is more or less unchanged in the investigated range of temperatures and the direct effect of temperature on the glucose spectrum is negligible compared to the influence of water. For samples where a small depth of penetration is sufficient, the region between 1100 and 1000 cm^{-1} is well suited for quantitative analysis. In this range, the glucose signals are at a maximum and temperature-dependent changes in the water spectrum are at a minimum. This region also shows promise for measurement of phosphates and sulfates in aqueous solutions under less controlled thermal conditions.

Near-Infrared Region. Figure 9 shows the subtraction of the pure water spectrum measured at 0.4 mm pathlength and 37 °C temperature from the 1 g/dL aqueous glucose spectrum measured at the same pathlength and temperature. Also shown is the difference spectrum of a 38 °C pure water spectrum with 37 °C water as reference. The addition of 1 g/dL glucose can be seen to have an influence on the underlying water spectrum that is equivalent to a change of 1 °C in temperature. The glucose-specific signals in the spectral region 4500–4200 cm^{-1} are a factor of 10 smaller than this matrix effect. Scaling this result to a typical glucose concentration of 100 mg/dL, reveals that the effect of this concentration is comparable to a temperature change of 0.1 °C. Moreover, the effect of the glucose signal itself is seen to be a factor of 10 smaller than that of the underlying water spectrum. This result indicates that baseline variations are introduced in the near-infrared spectrum when the glucose concentration changes, even when temperature is under strict control. No such matrix effects are observed in the mid-infrared region. This matrix effect suggests that the quantification of glucose from the near-infrared combination band requires a baseline correction even in situations where temperature is well controlled.

The effect of glucose on the temperature dependency of the underlying water absorption spectrum is further illustrated in Fig. 10, which shows the first loading vector resulting from a PCA analysis of pure water in the temperature range 36 to 42 °C and the first loading vector resulting from a separate PCA analysis of the 1 g/dL aqueous glucose in the same temperature range. These two loading vectors differ in shape, in particular around the absorption bands of water, showing that water absorption varies differently with temperature as glucose is added. The change in the water absorption with the addition of glucose is not merely an offset depending on the glucose concentration. Once again, this effect is small in the 4500–4200 cm^{-1} region containing combination bands of glucose. The glucose-specific signals in this region do not show up in the 1 g/dL glucose loading vector, indicating that these signals do not change with temperature.

A summary of the above results is given in Table III, which compares the spectral regions 1200–1000 and 5000–4000 cm^{-1}. The effect of temperature and the uncertainty of the measurements are nearly equal in the two spectral regions. In contrast, the absorbance of pure water is almost three times higher and the glucose signal is seen to be two orders of magnitude higher in the mid-infrared region. In the near-infrared region, matrix effects from the interaction between water and glucose are stronger than the glucose signal itself by an order of magnitude. The mutarotation of glucose is found to have little influence on the spectra, with a change of 0.3% when temperature changes by 1 °C in the mid-infrared region. No such change is observed in the near-infrared region. The above results indicate that the mid-infrared spectral region is better suited to quantification of glucose under

TABLE III. Comparison between the spectral regions 1200–1000 and 5000–4000 cm^{-1}. The data shown are the absorbance of pure water (column 1), the change in absorbance with a temperature change of 1 °C (column 2), the uncertainty of the measurement (column 3), the absorbance of aqueous glucose with pure water as reference (column 4), the change in glucose absorbance with a temperature change of 1 °C (column 5), and the change in underlying water absorbance with addition of glucose (column 6). All values are in absorbance units. The pathlengths for the mid- and near-infrared data were 50 μm and 0.4 mm, respectively.

	Pure water			100 mg/dL aqueous glucose		
Spectral region	Absorb.	ΔT = 1 °C	Uncertainty	Absorb.	ΔT = 1 °C	Matrix effect
1200–1000 cm^{-1}	1.2	6×10^{-4}	1.6×10^{-3}	9×10^{-3}	3×10^{-5}	NO
5000–4000 cm^{-1}	0.44	8×10^{-4}	1.5×10^{-3}	7×10^{-5}	NO	5×10^{-4}

circumstances where a short pathlength is possible. A short pathlength is certainly possible in making laboratory measurements. When it comes to noninvasive diagnostics, however, it may be difficult to find a suitable measurement site at which mid-infrared spectroscopy may be employed.

CONCLUSION

An accurate determination of the influence of variation in physiologically relevant temperatures on the spectrum of pure water was carried out in the mid- and near-infrared regions. Water absorption spectra were compared with existing reference spectra and changes in temperature with 37 °C water as reference were tabulated. The temperature was controlled within 0.02 °C, compared with typical accuracies of 0.1 °C in other studies. The limitations that changes in the pure water absorption spectrum impose on the quantification of trace components in aqueous solutions when temperature variations exist was discussed. The influence of temperature on a 1 g/dL aqueous glucose solution was studied. In the mid-infrared region, the variation of the spectrum was dominated by the change of the water spectrum alone, and the addition of glucose did not significantly change the underlying water spectrum. The glucose spectrum itself was found to change only weakly. This change was explained by a change in the equilibrium between the α and β form of glucose with temperature. In the near-infrared region, the addition of 1 g/dL glucose to pure water caused the underlying water spectrum to change. This change prevented successful subtraction of a pure water reference in order to isolate glucose signals and suggests that baseline correction by Fourier high-pass filtering may be necessary even when temperature is under control.

ACKNOWLEDGMENTS

The authors are grateful to the DANAK accredited temperature calibration facility at Risø National Laboratory for help with the thermostation of the transmission cell. This work has been carried out under grant no. RK930.9750.0006.0035.0092.0 from the Danish Research Academy and has received financial support from the Danish Center for Biomedical Optics and New Laser Systems.

1. S. Venyaminov and F. G. Prendergast, Anal. Biochem. **248,** 234 (1997).
2. H. L. Mark and P. R. Griffiths, Appl. Spectrosc. **56,** 633 (2002).
3. Y. Houdas and E. F. J. Ring, *Human Body Temperature: Its Measurements and Regulation* (Plenum Press, New York, 1982).
4. T. M. Blank, T. L. Ruchti, S. F. Malin, and S. L. Monfre, LEOS Newsletter **13,** 9 (1999).
5. H. M. Heise and R. Marbach, Cell. Mol. Biol. **44,** 899 (1999).
6. J. J. Burmeister and M. A. Arnold, Clin. Chem. **45,** 1621 (1999).
7. M. R. Robinson, Robust accurate non-invasive analyte monitor. Patent 5830132, U.S. Patent (1998).
8. K. J. Ward, D. M. Haaland, M. R. Robinson, and R. P. Eaton, Appl. Spectrosc. **46,** 959 (1992).
9. A. Welch and M. van Gemert, *Optical-Thermal Response of Laser-Irradiated Tissue* (Plenum Press, New York, 1995).
10. J. E. Bertie and Z. Lan, Appl. Spectrosc. **50,** 1047 (1996).
11. F. O. Libnau, J. Toft, A. A. Christy, and O. M. Kvalheim, J. Am. Chem. Soc. **116,** 8311 (1994).
12. F. O. Libnau, O. M. Kvalheim, A. A. Christy, and J. Toft, Vib. Spectrosc. **7,** 243 (1994).
13. K. Rahmelow and W. Hübner, Appl. Spectrosc. **51,** 160 (1997).
14. J. J. Kelly, K. A. Kelly, and C. H. Barlow, Proc. SPIE-Int. Soc. Opt. Eng. **2389,** 818 (1995).
15. K. H. Hazen, M. A. Arnold, and G. W. Small, Appl. Spectrosc. **48,** 477 (1994).
16. J. E. Bertie, in *Analytical Applications of FT-IR to Molecular and Biological Systems,* J. R. Durig, Ed. (D. Reidel Publishing Company, Dordrecht: Holland, 1980), vol. 57 of *NATO Advanced Study Institutes, Series C—Mathematical and Physical Sciences.*
17. W. H. Press, S. A. Teukolsky, W. T. Vetterling, and B. P. Flannery, *Numerical Recipes in C The Art of Scientific Computing* (Cambridge University Press, Cambridge, 1995), 2nd ed.
18. H. Martens and T. Næs, *Multivariate Calibration* (John Wiley and Sons, New York, 1989).
19. S. Wold, K. Esbensen, and P. Geladi, Chemom. Intell. Lab. Syst. **2,** 37 (1987).
20. K. F. Palmer and J. Williams, J. Opt. Soc. Am. **64,** 1107 (1974).
21. K. H. Hazen, M. A. Arnold, and G. W. Small, Appl. Spectrosc. **52,** 1597 (1998).
22. F. O. Libnau, A. A. Christy, and O. M. Kvalheim, Vib. Spectrosc. **7,** 139 (1994).
23. J. C. Kendrew and E. A. Molwyn-Hughes, Proc. R. Soc. London, Ser. A **176,** 352 (1940).